

# Application of Bounded Total Variation Denoising in Urban Traffic Analysis

Shanshan Tang<sup>a,b</sup>, Haijun Yu<sup>b,a</sup>

<sup>a</sup>*School of Mathematical Sciences, University of Chinese Academy of Sciences, Beijing 100049, China*  
<sup>b</sup>*NCMIS & LSEC, Institute of Computational Mathematics and Scientific/Engineering Computing, Academy of Mathematics and Systems Science, Beijing 100190, China*

---

## Abstract

While it is believed that denoising is not always necessary in many big data applications, we show in this paper that denoising is helpful in urban traffic analysis by applying the method of bounded total variation denoising to the urban road traffic prediction and clustering problem. We propose two easy-to-implement methods to estimate the noise strength parameter in the denoising algorithm, and apply the denoising algorithm to GPS-based traffic data from Beijing taxi system. For the traffic prediction problem, we combine neural network and history matching method for roads randomly chosen from an urban area of Beijing. Numerical experiments show that the predicting accuracy is improved significantly by applying the proposed bounded total variation denoising algorithm. We also test the algorithm on clustering problem, where a recently developed clustering analysis method is applied to more than one hundred urban road segments in Beijing based on their velocity profiles. Better clustering result is obtained after denoising.

*Keywords:* Urban traffic prediction, Bounded variation denoising, Noise estimate, Clustering

---

## 1. Introduction

Transportation has become an important part in our daily life, which brings many kinds of traffic problems at the same time. For example, big cities like Beijing have a trend to be more and more congested as the enormous growing of private cars. Many researchers have tried to analysis and alleviate the traffic congestion problem with different methods, especially using vehicle GPS (Global Positioning System) trajectories as more and more data are available. There are researches exploring the cause and propagation of traffic jams [1, 2], mining the fastest driving route [3], trying clustering methods for trajectories to characterize patterns of traffic [4, 5], estimating the volume of citywide transportation [6], predicting the taxi destinations [7] and forecasting traffic velocity [8, 9]. All of these works are based on trajectories and have utilized temporal, spatial or spatio-temporal properties. In this paper, we are interested in urban traffic velocity prediction. As we all know if the velocity is much lower than the average velocity of a road for a relatively long time, then there is a high possibility that congestion is formed. So if the traffic velocity of a road can be predicted accurately on the base of historical data, then it will be very helpful for routine planning, congestion control and analysis, etc.. However, such a traffic forecast is not an easy task in practice as a result of both the limit of methods and data volume and quality. Urban traffic is a quite complex system, leading that data collected contain noises. Noises may come from two aspects. On one hand, due to the number of cars appearing on a given urban road segment in a short time interval is very limited, one need to consider the average number of cars and the average velocity on a given road as stochastic processes. On the other hand, measurement error and other error may be introduced in the data collection and post-processing procedures. Correspondingly, there are two ways to deal with noisy data. One is to treat noise as real, and develop new methods to improve accuracy(see, e.g., [8, 9, 7, 4, 5]). The other is to first reduce noise in the collected data [10], and then use the denoised data to forecast on the base of existing methods [11, 12].

In this paper, we prefer to the latter way mentioned above. The reasons are as follows. First, data can be used in urban traffic analysis without expensive cost comparing to the complexity of the

problem are often limited, so we need to make the limited data effective rather than using the noisy data directly. Second, although some existing and latest methods have some tolerance with noise, like deep neural network [13, 14], the real performance of the network depends on many factors and we believe these methods will perform better with proper-denoised data under the same condition. Third, by using dedicated denoising algorithms, shallow neural networks using less data can give fairly good urban traffic prediction, which is favorable in real-time and online applications comparing to deep neural networks due to its efficiency.

There exist many useful methods developed for image and video denoising, such as [15, 16, 17, 18, 19, 20, 21]. Some of these methods have been applied to traffic analysis, e.g. the wavelet method [11, 22] and the compressive sensing method [10, 23, 12]. These methods work fairly well in some denoising applications, but they are based on assumptions on noise and specific basis functions. We want to find a method works well without any assumptions on noise and basis functions when denoising and the parameters of which are easy to obtain. Thus we propose to apply bounded total variation (BV) denoising method [19] to urban traffic velocity data. It is a nonlinear and edge preserving method [24], which is consistent with the sudden jump existing in traffic velocities, and suggested by [12]. Our goal is to find the reconstructed velocity vector in the function space of bounded total variation and estimate the noise strength during the process of denoising without any special assumption on the type of noise. To this end, we propose two efficient methods to estimate the noise strength, which almost do not request any assumptions on noise, and apply the resulting BV denoising algorithm to urban GPS-based traffic data from Beijing taxi system, to improve the accuracy of traffic prediction and cluster analysis.

In the following section, we first review the method of BV denoising, then show how to apply the BV denoising method to traffic data by proposing two efficient ways to estimate the noise strength. After that, we validate the effectiveness of denoising by applying it to real urban data from Beijing taxi system. A brief conclusion is given at the end of this paper.

## 2. The BV denoising algorithm for traffic velocity data

In this section, we first review the method of BV denoising, and then show how to apply it to traffic velocity data.

### 2.1. The continuous BV denoising model

Let  $u_0(x)$ ,  $x \in \Omega \subseteq \mathbf{R}^d$  be the original observed velocity vector and  $u(x)$  be the denoised velocity vector, then we have  $u_0(x) = u(x) + \xi(x)$ , where  $\xi(x)$  is the noise whose mean is 0. We first consider the BV denoising method for the continuous case and then discuss the corresponding discrete case. Assume  $u$  is smooth, the BV denoising method is to find the solution of the following optimization problem [19]

$$\min_{u(x)} \text{TV}(u) = \min_{u(x)} \int_{\Omega} |\nabla u(x)| dx, \quad (1)$$

such that

$$\int_{\Omega} u(x) dx = \int_{\Omega} u_0(x) dx, \quad \frac{1}{2} \int_{\Omega} (u(x) - u_0(x))^2 dx = \sigma^2. \quad (2)$$

When we apply the BV denoising method to reduce the noise in road velocity time series,  $x$  is a one dimensional vector, so we only consider the case that  $d = 1$  below. The first order necessary condition of the optimization problem satisfies (2) and following Euler-Lagrange equation:

$$\frac{d}{dx} \left( \frac{u_x}{|u_x|} \right) - \lambda_1 - \lambda_2(u - u_0) = 0, \quad \frac{\partial u}{\partial n} \Big|_{\partial\Omega} = 0,$$

where  $u_x = \frac{\partial u}{\partial x}$ ,  $\lambda_1$  and  $\lambda_2$  are the corresponding Lagrange multipliers. To obtain the solution of the optimization problem (1)-(2), one can solve the following equations, which correspond to the gradient flow of the Lagrange function with respect to  $u$ :

$$u_t = \frac{d}{dx} \left( \frac{u_x}{|u_x|_{\epsilon}} \right) - \lambda_2(u - u_0), \quad (3)$$

$$\frac{\partial u}{\partial n} \Big|_{\partial\Omega} = 0, \quad (4)$$

$$u(x, 0) = u_0(x) + \sigma\phi, \quad (5)$$

where  $\phi$  in (5) satisfies  $\mathbb{E}(\phi) = 0$ ,  $\frac{1}{2} \int_{\Omega} \phi^2 dx = 1$  such that  $u(x, 0)$  satisfies the constraint (2), and  $\epsilon$  is a relatively small positive number with  $|x|_{\epsilon} = |x| + \epsilon$  to avoid singularity and obtain better numerical stability. In addition, when initial condition like (5) is used, we can assure  $\lambda_1 = 0$  all the time. So we discard  $\lambda_1$  and only keep  $\lambda_2$ . For simplification, we set  $\lambda = \lambda_2$ . Now we calculate  $\lambda$ . Multiply  $u(x) - u_0(x)$  on both sides of (3), integrate on  $\Omega$  at the same time, and combine the Neumann boundary condition and (2), suppose  $u_t = 0$ , we obtain a formula for  $\lambda$ :

$$\lambda = \frac{1}{2\sigma^2} \int_{\Omega} \frac{u_x}{|u_x|_{\epsilon}} \cdot ((u_0)_x - u_x) dx. \quad (6)$$

$\lambda$  changes as  $u_x$  changes with respect to  $t$ , and converges when  $t$  is approaching infinity [19, 25].

If the steady state solution of (3)-(4) is obtained, it can be regarded as the clean data denoised from the observed data  $u_0(x)$ . Next, we present numerical schemes to solve the equations (3)-(4) in discrete case.

## 2.2. The discrete projected gradient descent algorithm

The data we have are average traffic velocities on urban roads derived from the taxi GPS trajectories. If we have a velocity record for every 5 minute period, then we have 288 records for each road every day. However, the velocity records are often less than 288 for most roads because of the limit of taxi numbers and recording equipments. Therefore, we make nearest interpolation for missing values for each road such that each road has 288 velocity records each day. In this way, we can set  $N = 288$ , and let  $x$  direction correspond to direction of  $N$  time slices for a road when making a numerical calculation. Define

$$\sigma_d^2 = \frac{1}{2} \sum_{i=1}^N (u(x_i) - u_0(x_i))^2 \cdot h, \quad (7)$$

where  $h$  is the duration of time intervals in which the traffic velocity on road segments are averaged. For the data we used,  $h$  is 5 minutes.  $x_i = ih$ ,  $i = 1, 2, \dots, N$  are the time intervals in one day,  $u_0(x_i)$ ,  $u(x_i)$  are the observed and denoised velocity for time slice  $i$ ,  $\sigma_d$  corresponds to the noise strength in discrete case. While  $\sigma$  and  $\sigma_d$  are different, we do not distinguish them in the following for convenience.

We use projected gradient descent method [25] to find the numerical solution of equations (3)-(5) because it is easy to implement and is guaranteed that the iteration converges to the solution we want [26]. Denote  $[N] = \{1, 2, \dots, N\}$ . Let  $u_i^n = u(x_i, \Delta t^n)$ ,  $\Delta^+ u_i^n = u_{i+1}^n - u_i^n$  for  $i \in [N]$ , where  $n$  is the iteration index,  $\Delta t^n$  is the step size of the  $n$ -th iteration. The detailed discrete projected gradient descent bounded variation denoising (PGDBV) algorithm is described as follows.

**Algorithm PGDBV:** The algorithm takes the observed velocity series:  $\{u_0(x_i), i = [N]\}$ ; the variance of the noise:  $\sigma$ ; the maximum iteration number:  $N_{iter}$ ; the relative tolerance of gradient decay:  $\delta$ ; as *input*. The *output*: denoised velocity series:  $\{u_i, i = [N]\}$ ; and the total variation of denoised data:  $V$ ; are calculated by performing the following steps.

1. Initialize velocity series:  $u_i^0 = u_0(x_i)$ ,  $i = [N]$ , and calculate the initial discrete total variation:

$$V^n = \text{TV}(u^n) = \sum_{i=1}^{N-1} |u_{i+1}^n - u_i^n|, \quad (8)$$

with  $n = 0$ .

2. For  $n$  from 0 to  $N_{iter} - 1$ , do the following iterations
  - (a) Update the Lagrange multiplier  $\lambda^n$  as

$$\lambda^n = \frac{1}{2\sigma^2} \sum_{i=1}^{N-1} \frac{\Delta^+ u_i^n}{|\Delta^+ u_i^n|_{\epsilon}} (\Delta^+(u_0)_i - \Delta^+ u_i^n);$$

(b) calculate the gradient of the  $i$ -th segment as

$$g_i^n = -\left(\frac{1}{h}\left(\frac{\Delta^+ u_i^n}{|\Delta^+ u_i^n|_\epsilon} - \frac{\Delta^+ u_{i-1}^n}{|\Delta^+ u_{i-1}^n|_\epsilon}\right) - \lambda^n(u_i^n - u_0(x_i))\right), \quad \text{for } i = [N],$$

where  $\Delta^+ u_0^n = 0$ , and  $\Delta^+ u_{N-1}^n = 0$ .

(c) Obtain step size  $\Delta t^n$  with line search;

(d) Update the variable  $u^{n+1} = u^n - \Delta t^n g^n$ ;

(e) Calculate the total variation  $V^{n+1}$  using (8) with  $n$  replaced by  $n+1$ ;

(f) If  $\|g^n\|_\infty/V^0 \leq \delta$ , then set  $u_i = u_i^{n+1}$  for  $i = [N]$  and  $V = V^{n+1}$ , and return.

3. Set  $u_i = u_i^{N_{iter}}$  for  $i = [N]$  and  $V = V^{N_{iter}}$ , and return.

### 2.3. Estimate of the noise strength

In the denoising algorithm given in Algorithm PGDBV, we regard  $\sigma$  as a constant, which is a characterization of the noise strength. But we do not know its value a priori. Now we propose two different ways to estimate the noise strength.

**Method 1:** multi-resolution noise estimate

In each day, every road has  $N = 288$  velocity records corresponding to  $N$  time slices. We want to estimate the noise strength in three different resolutions. Let  $N_1 = N$ ,  $N_2 = \frac{N}{2}$ ,  $N_3 = \frac{N}{4}$ . Let  $u_0^0(x_i) = u_0(x_i)$  for  $i \in [N_1]$  and

$$u_0^1(x_i) = \frac{u_0^0(x_{2i}) + u_0^0(x_{2i-1})}{2}, \quad i \in [N_2]; \quad u_0^2(x_i) = \frac{u_0^1(x_{2i}) + u_0^1(x_{2i-1})}{2}, \quad i \in [N_3].$$

Then the variation in three resolutions are:

$$V_{j+1} = \sum_{i=1}^{N_1-1} |u_0^j(x_{i+1}) - u_0^j(x_i)|^2 \cdot \frac{1}{2^j h}, \quad j = 0, 1, 2.$$

In order to estimate the noise strength, we give a lemma first.

**Lemma 1.** Let  $u_0(x_i) = u_i + \xi_i$ ,  $i \in [N]$ , where  $u_0(x_i)$ ,  $u_i$ ,  $\xi_i$  represent the observed, denoised data and noise for time slice  $i$  separately. Denote  $u_i^1 = \frac{u_{2i-1} + u_{2i}}{2}$ ,  $i \in [N_2]$ ,  $u_i^2 = \frac{u_{2i-1}^1 + u_{2i}^1}{2}$ ,  $i \in [N_3]$ ,  $h = \frac{T}{N}$ , where  $T$  is the time length, then the following relations satisfy:

$$\begin{aligned} \sum_{i=1}^{N_2} (u_i^1 - u_0^1(x_i))^2 &= \frac{1}{4} \sum_{i=1}^{N_1} (u_i - u_0(x_i))^2 + \frac{1}{2} \sum_{i=1}^{N_2} (u_{2i-1} - u_0(x_{2i-1}))(u_{2i} - u_0(x_{2i})), \\ \sum_{i=1}^{N_3} (u_i^2 - u_0^2(x_i))^2 &= \frac{1}{4} \sum_{i=1}^{N_2} (u_i^1 - u_0^1(x_i))^2 + \frac{1}{2} \sum_{i=1}^{N_3} (u_{2i-1}^1 - u_0^1(x_{2i-1}))(u_{2i}^1 - u_0^1(x_{2i})). \end{aligned}$$

*Proof.* 1) For the first equation, let  $h_2 = 2h$ , we have

$$\begin{aligned} &\sum_{i=1}^{N_2} (u_i^1 - u_0^1(x_i))^2 \cdot h_2 \\ &= \sum_{i=1}^{N_2} \left( \frac{u_{2i} + u_{2i-1}}{2} - \frac{u_0(x_{2i}) + u_0(x_{2i-1})}{2} \right)^2 \cdot 2h \\ &= \sum_{i=1}^{N_2} \left( \frac{u_{2i} - u_0(x_{2i})}{2} + \frac{u_{2i-1} - u_0(x_{2i-1})}{2} \right)^2 \cdot 2h \\ &= \frac{h}{2} \sum_{i=1}^{N_1} (u_i - u_0(x_i))^2 + h \sum_{i=1}^{N_2} (u_{2i} - u_0(x_{2i}))(u_{2i-1} - u_0(x_{2i-1})) \end{aligned}$$

Rearrange the equation above and then the formula for  $\sum_{i=1}^{N_2} (u_i^1 - u_0^1(x_i))^2$  is obtained.

2) For the second equation, let  $h_3 = 4h$ , the proof can be done using similar procedure.  $\square$

Making use of Lemma 1, we can obtain the estimate of  $\sigma$ , denoted by  $\hat{\sigma}$ .

**Theorem 1.** Assume  $\xi_i$  is independent with  $\xi_j$  for  $i \neq j$ ,  $\mathbb{E}(\xi_i) = 0$ ,  $\mathbb{E}(\xi_i^2) = \frac{2\sigma^2}{Nh}$ ,  $i \in [N]$ , then

$$\hat{\sigma}^2 = h^2 \frac{\left(\frac{119}{16} - \frac{27}{4N}\right)V_1 + \left(\frac{9}{4N} - \frac{49}{16}\right)V_2 + \left(\frac{9}{2N} - \frac{35}{8}\right)V_3}{\frac{3577}{128} + \frac{189}{8N^2} - \frac{819}{16N}}. \quad (9)$$

This estimation is consistent, in the sense that,

$$\mathbb{E}(\hat{\sigma}^2) - \sigma^2 = h^2 \frac{\left(\frac{49}{16} - \frac{9}{4N}\right)(V_1^c - V_2^c) + \left(\frac{35}{8} - \frac{9}{2N}\right)(V_1^c - V_3^c)}{\frac{3577}{128} + \frac{189}{8N^2} - \frac{819}{16N}}, \quad (10)$$

where

$$V_1^c = \sum_{i=1}^{N_1-1} \frac{|u_{i+1} - u_i|^2}{h}, \quad V_j^c = \sum_{i=1}^{N_j-1} \frac{|u_{i+1}^{j-1} - u_i^{j-1}|^2}{2^{j-1}h}, \quad \text{for } j = 2, 3.$$

*Proof.* We prove this theorem in three steps.

(1) By definition of  $V_1$ , we get

$$V_1 = \frac{1}{h} \left( 2 \sum_{i=1}^{N_1} (u_0(x_i))^2 - (u_0(x_1))^2 - (u_0(x_{N_1}))^2 - 2 \sum_{i=1}^{N_1-1} u_0(x_i)u_0(x_{i+1}) \right).$$

We get the representation for  $\sum_{i=1}^{N_1} (u_0(x_i))^2$  from equation (7), leading that

$$V_1 = \frac{4\sigma^2}{h^2} + \frac{1}{h} \left( 4 \sum_{i=1}^{N_1} u_i u_0(x_i) - 2 \sum_{i=1}^{N_1} (u_i)^2 - (u_0(x_1))^2 - (u_0(x_{N_1}))^2 - 2 \sum_{i=1}^{N_1-1} u_0(x_i)u_0(x_{i+1}) \right).$$

Similarly, combine the definition of  $V_2$ ,  $V_3$  and Lemma 1, we obtain the representation of  $V_2$  and  $V_3$

$$\begin{aligned} V_2 &= \frac{\sigma^2}{2h^2} + \frac{1}{2h} \left( \sum_{i=1}^{N_2} (u_{2i-1} - u_0(x_{2i-1}))(u_{2i} - u_0(x_{2i})) \right. \\ &\quad \left. + 4 \sum_{i=1}^{N_2} u_i^1 u_0^1(x_i) - 2 \sum_{i=1}^{N_2} (u_i^1)^2 - (u_0^1(x_1))^2 - (u_0^1(x_{N_2}))^2 - 2 \sum_{i=1}^{N_2-1} u_0^1(x_i)u_0^1(x_{i+1}) \right), \\ V_3 &= \frac{\sigma^2}{16h^2} + \frac{1}{4h} \left( \frac{1}{4} \sum_{i=1}^{N_2} (u_{2i-1} - u_0(x_{2i-1}))(u_{2i} - u_0(x_{2i})) \right. \\ &\quad \left. + \sum_{i=1}^{N_3} (u_{2i-1}^1 - u_0^1(x_{2i-1}))(u_{2i}^1 - u_0^1(x_{2i})) \right. \\ &\quad \left. + 4 \sum_{i=1}^{N_3} u_i^2 u_0^2(x_i) - 2 \sum_{i=1}^{N_3} (u_i^2)^2 - (u_0^2(x_1))^2 - (u_0^2(x_{N_3}))^2 - 2 \sum_{i=1}^{N_3-1} u_0^2(x_i)u_0^2(x_{i+1}) \right). \end{aligned}$$

(2) Now, we are ready to apply the assumptions in the theorem.

After regrouping the order of the representation of  $V_1, V_2, V_3$  and replacing  $u_0(x_i)$  with  $u_i + \xi_i$ , we obtain

$$\begin{aligned} V_1 &= \frac{2}{h} \sum_{i=1}^{N_1-1} ((u_{i+1} - u_i)(\xi_{i+1} - \xi_i) - \xi_i \xi_{i+1}) + \frac{4\sigma^2}{h^2} - \frac{\xi_1^2}{h} - \frac{\xi_{N_1}^2}{h} + \sum_{i=1}^{N_1-1} (u_i - u_{i+1})^2 \frac{1}{h}, \\ V_2 &= \frac{\sigma^2}{2h^2} + \frac{1}{2h} \left( \sum_{i=1}^{N_2} \xi_{2i-1} \xi_{2i} - \left( \frac{\xi_1 + \xi_2}{2} \right)^2 - \left( \frac{\xi_{N_1-1} + \xi_{N_1}}{2} \right)^2 \right) \end{aligned}$$

$$\begin{aligned}
& + \sum_{i=1}^{N_2-1} \left( (u_{i+1}^1 - u_i^1)(\xi_{2i+1} + \xi_{2i+2} - \xi_{2i-1} - \xi_{2i}) - \frac{(\xi_{2i-1} + \xi_{2i})(\xi_{2i+1} + \xi_{2i+2})}{2} \right) \\
& + \sum_{i=1}^{N_2-1} (u_{i+1}^1 - u_i^1)^2, \\
V_3 = & \frac{\sigma^2}{16h^2} + \frac{1}{4h} \left( \frac{1}{4} \sum_{i=1}^{N_2} \xi_{2i-1} \xi_{2i} + \sum_{i=1}^{N_3} \frac{(\xi_{4i-3} + \xi_{4i-2})(\xi_{4i-1} + \xi_{4i})}{4} \right. \\
& - \frac{(\sum_{i=1}^4 \xi_i)^2 + (\sum_{j=0}^3 \xi_{N_1-j})^2}{16} + \sum_{i=1}^{N_3-1} (u_i^2 - u_{i+1}^2)^2 \\
& \left. + \sum_{i=1}^{N_3-1} \left( \frac{(u_{i+1}^2 - u_i^2)(\sum_{j=1}^4 (\xi_{4i+j} - \xi_{4i+1-j}))}{2} - \frac{(\sum_{j=0}^3 \xi_{4i-j})(\sum_{j=1}^4 \xi_{4i+j})}{8} \right) \right).
\end{aligned}$$

Take expectation on the equations above and combine the assumptions, then

$$\begin{aligned}
\mathbb{E}(V_1) &= (4 - \frac{4}{N}) \frac{\sigma^2}{h^2} + \sum_{i=1}^{N_1-1} (u_{i+1} - u_i)^2 \cdot \frac{1}{h}, \\
\mathbb{E}(V_2) &= (\frac{1}{2} - \frac{1}{N}) \frac{\sigma^2}{h^2} + \sum_{i=1}^{N_2-1} (u_{i+1}^1 - u_i^1)^2 \cdot \frac{1}{2h}, \\
\mathbb{E}(V_3) &= (\frac{1}{16} - \frac{1}{4N}) \frac{\sigma^2}{h^2} + \sum_{i=1}^{N_3-1} (u_{i+1}^2 - u_i^2)^2 \cdot \frac{1}{4h}.
\end{aligned}$$

From what have done above, we can estimate  $\sigma$  by fitting a line with 3 points:  $(4 - \frac{4}{N}, V_1), (\frac{1}{2} - \frac{1}{N}, V_2), (\frac{1}{16} - \frac{1}{4N}, V_3)$ . The slope of the line is  $\frac{\sigma^2}{h^2}$ , then  $\sigma$  is estimated.

(3) Estimate the value of  $\sigma$ . Set

$$X_1 = 4 - \frac{4}{N}, \quad X_2 = \frac{1}{2} - \frac{1}{N}, \quad X_3 = \frac{1}{16} - \frac{1}{4N},$$

and assume  $(X_1, V_1), (X_2, V_2), (X_3, V_3)$  satisfy

$$V_i = AX_i + b + \mu_i, \quad i = 1, 2, 3,$$

where  $\mu_i$  means the random disturbance variables.

Then we want to fit a line with these 3 points, which is

$$V = \hat{A}X + \hat{b}.$$

With the help of least square method, we obtain the representation of  $\hat{A}$  as follows:

$$\hat{A} = \frac{3 \sum_{i=1}^3 X_i V_i - \sum_{i=1}^3 X_i \sum_{i=1}^3 V_i}{3 \sum_{i=1}^3 X_i^2 - (\sum_{i=1}^3 X_i)^2}. \quad (11)$$

So we estimate  $\sigma^2$  by

$$\hat{\sigma}^2 = h^2 \frac{(\frac{119}{16} - \frac{27}{4N})V_1 + (\frac{9}{4N} - \frac{49}{16})V_2 + (\frac{9}{2N} - \frac{35}{8})V_3}{\frac{3577}{128} + \frac{189}{8N^2} - \frac{819}{16N}}.$$

Combine the assumption  $V_i = AX_i + b + \mu_i, i = 1, 2, 3$ , and (11), we get

$$\hat{A} = A + \frac{3 \sum_{i=1}^3 X_i \mu_i - \sum_{i=1}^3 X_i \sum_{i=1}^3 \mu_i}{3 \sum_{i=1}^3 X_i^2 - (\sum_{i=1}^3 X_i)^2}. \quad (12)$$

Thus,

$$\mathbb{E}(\hat{A}) = A + \frac{3 \sum_{i=1}^3 X_i \mathbb{E}(\mu_i) - \sum_{i=1}^3 X_i \sum_{i=1}^3 \mathbb{E}(\mu_i)}{3 \sum_{i=1}^3 X_i^2 - (\sum_{i=1}^3 X_i)^2}. \quad (13)$$

Notice that by the construct of  $V_i$  and the linear assumption for  $V_i, i = 1, 2, 3$ , the following relations are established:

$$\begin{aligned} b + \mu_1 &= \sum_{i=1}^{N_1-1} |u_{i+1} - u_i|^2 \cdot \frac{1}{h} = V_1^c, \\ b + \mu_2 &= \sum_{i=1}^{N_2-1} |u_{i+1}^1 - u_i^1|^2 \cdot \frac{1}{2h} = V_2^c, \\ b + \mu_3 &= \sum_{i=1}^{N_3-1} |u_{i+1}^2 - u_i^2|^2 \cdot \frac{1}{4h} = V_3^c. \end{aligned}$$

Substitute  $\mathbb{E}(\mu_i) = V_i^c - b$  into (13), we derive

$$\mathbb{E}(\hat{A}) = A + \frac{(\frac{49}{16} - \frac{9}{4N})(V_1^c - V_2^c) + (\frac{35}{8} - \frac{9}{2N})(V_1^c - V_3^c)}{\frac{3577}{128} + \frac{189}{8N^2} - \frac{819}{16N}}.$$

Denote

$$Bias(N) = h^2 \frac{(\frac{49}{16} - \frac{9}{4N})(V_1^c - V_2^c) + (\frac{35}{8} - \frac{9}{2N})(V_1^c - V_3^c)}{\frac{3577}{128} + \frac{189}{8N^2} - \frac{819}{16N}}. \quad (14)$$

Because  $\hat{A} = \frac{\hat{\sigma}^2}{h^2}$ ,  $A = \frac{\sigma^2}{h^2}$ , we get equation (10).  $\square$

From the representation of  $\mathbb{E}(\hat{\sigma}^2)$  in Theorem 1, it can be seen that  $\hat{\sigma}$  depends on  $h$ . The difference between  $\sigma$  and  $\hat{\sigma}$  is of order  $h$ .

We test two examples to check the ability of the method proposed above: 1)  $u(x) = \sin(\pi x)$ ,  $x = [-1, 1]$ ,  $h = \frac{2}{N}$ ; 2)  $u(x) = \max(1 - |x|, 0)$ ,  $x = [-1, 1]$ ,  $h = \frac{2}{N}$ . We add white noise whose standard deviation is  $\sigma$  such that the signal-to-noise ratio is 3. Test results are in Table 1. From Table 1, we found that the numerical results of proposed method for estimating  $\sigma$  are very good. However, some assumptions on noise are required in this method. Next, we present a method use less assumptions.

Table 1: Numerical Results of Noise Estimate using Method 1.

	$u(x) = \sin(\pi x)$			$u(x) = \max(1 -  x , 0)$		
$N_l$	288	144	72	288	144	72
$\sigma$	0.4941	0.4446	0.4385	0.4127	0.4176	0.3992
$\hat{\sigma}$	0.4896	0.4558	0.4646	0.4089	0.4290	0.3813
$Bias(N_l)$	2e-6	1.69e-5	1.47e-4	4.47e-7	3.59e-6	2.89e-5
$\hat{\sigma}^2/\sigma^2 - 1$	-0.0182	0.0508	0.1230	-0.0182	0.0554	-0.0878

**Method 2:** a balance between  $\sigma$  and  $TV$

From the BV algorithm, we see that when  $\sigma = 0$ ,  $TV = TV(u_0)$ . If we increase  $\sigma$  from 0,  $TV$  decreases. As  $\sigma$  get larger and larger,  $TV$  decrease to 0. In the process, a critical point at which the decreasing speed of  $TV$  has a relatively slow-down exists. We regard this point as  $\hat{\sigma}$ , and give a quantitative way to identify  $\hat{\sigma}$  below. Choose some values for  $\sigma$  in increasing order first. And for any two successive  $\sigma_1$  and  $\sigma_2$ ,  $\sigma_1 < \sigma_2$ , calculate the variance  $\delta(TV(\sigma_2) \cdot \sigma_2^2)$  as

$$\delta(TV(\sigma_2) \cdot \sigma_2^2) = TV(\sigma_2) \cdot \sigma_2^2 - TV(\sigma_1) \cdot \sigma_1^2. \quad (15)$$

Plot the relation figure for  $\delta(TV(\sigma) \cdot \sigma^2)$  and  $\sigma^2$ , where  $\sigma$  is from the chosen values at first. Then find the  $\sigma$  where  $\delta(TV(\sigma) \cdot \sigma^2)$  reaches minimum value for the first time, and regard it as the value for  $\hat{\sigma}$ .

We have presented two methods to estimate noise strength  $\hat{\sigma}$ . However, both of them have advantages and disadvantages. The first method can be calculated directly and easily, but the estimation result depends on some related assumptions. The second method does not need any assumption on noise, but it is heuristic. To get a better estimate, we combine the two methods together. Let  $\hat{\sigma}_1, \hat{\sigma}_2$  denote the estimated noise strength with **Method 1** and **2**. Denote the maximum, minimum velocity for a road in a day by  $v_{\max}, v_{\min}$ , correspondingly. Then take  $TV_l = \frac{5}{2}(v_{\max} - v_{\min})$  as a lower bound of  $TV$ . If the  $TV$  corresponding to  $\min(\hat{\sigma}_1, \hat{\sigma}_2)$  is less than  $TV_l$ , then let  $\hat{\sigma}$  be the  $\sigma$  corresponding to  $TV_l$ , otherwise  $\hat{\sigma} = \min(\hat{\sigma}_1, \hat{\sigma}_2)$ .

### 3. Experiments

In this section, we use real taxi GPS data of Beijing to demonstrate the performance of our method. There are 288 five-minute time slices one day. If no GPS record appears in some five-minute, we get no velocity record in that time slice. In general, if one method performs well in a randomly chosen domain of Beijing, then it can be extended to other domains. Therefore, we randomly choose an area from Beijing and consider the GPS records for roads in it. First, we choose 24 roads at random from this fixed domain, with road length not less than 100 meters and daily record number not less than 150. We use the 24 roads to test the estimated noise strength with methods proposed in last section and combine them together to obtain the best estimate. After that, the velocity of these 24 roads before and after denoising on a fixed day are presented to give a visual effect directly. In further, we use history matching to show that predicting accuracy is improved after denoising with the best estimated noise strength. Second, 102 roads in the chosen domain, whose length is not less than 100 meters and velocity records are not less than 120, are put together to see the denoising effect on clustering. As a result, a satisfactory clustering consequence is obtained after denoising. Note that, road segments in Beijing are divided into 6 types, which are Urban Express Highway, Freeway, National Highway, Provincial Highway, Prefectural Highway and Rural Street, corresponding to that road type value is from 1 to 6 respectively.

#### 3.1. Estimated best noise strength

We carry out experiments on the 24 roads for 8 days, and only present some related results on the first day in this part since the results of other 7 days are similar. Day 1 to 8 correspond to March 4-8, 18-19, 11, 2013, all of which are weekdays. We have mentioned that there are time slices without velocity record, for which we use linear nearest interpolation and matrix completion methods to complete the missing values. The contents of matrix completion are given in the last paragraph of the third part in this section. The estimated  $\sigma$  for the 24 roads on Day 1 with two different kinds of treatments for missing values by **Method 1** are shown in Figure 1, which reveals they are little difference. Then we

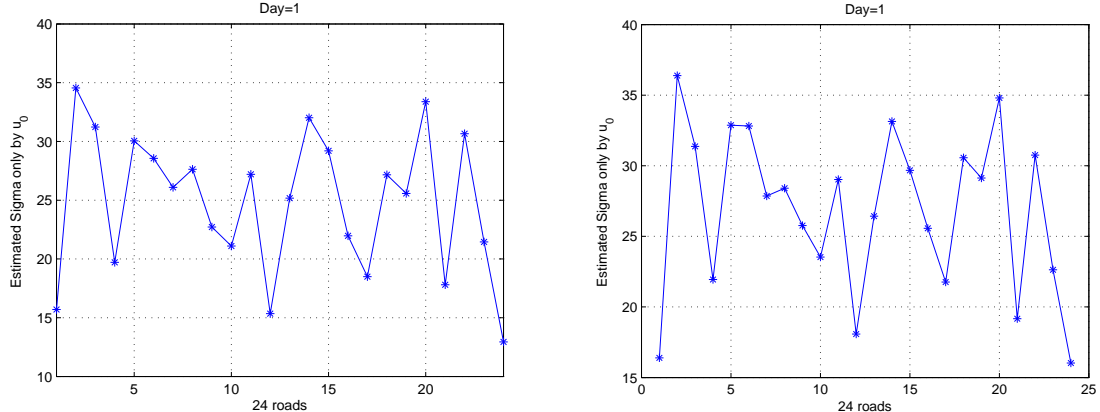


Figure 1: Estimated  $\sigma$  by **Method 1** using different methods for missing values (Left: Nearest interpolation; Right: Matrix completion).

estimate noise strength with **Method 2**. First, Figure 2 shows the relationship between  $TV$  and  $\sigma^2$ , where the horizontal and vertical axis represent  $\sigma^2$  and variance of  $TV$ . The values of  $\sigma$  are 0, 1 and every other 5 from 5 to 50, totally 12 numbers. In this figure, red star points correspond to the 12  $\sigma^2$ s, and blue star points denote the cases for  $\sigma^2 = [10^2, 20^2, 30^2]$ . It can be discovered that, for each road,  $TV$  is decreasing with the growth of  $\sigma^2$ . After choosing the values of  $\sigma$ , the quantitative way to identify  $\hat{\sigma}_2$  in Method 2 can be applied and is described in Figure 3, where the horizontal axis is the value of  $\sigma^2$ , and vertical axis is  $\delta(TV(\sigma) \cdot \sigma^2)$ . For example, the abscissa of the first point on road 1 is  $\sigma = 1$ , and its ordinate is  $\delta(TV(1) \cdot 1^2)$ .  $\hat{\sigma}_2$  is the location where  $\delta(TV(\sigma) \cdot \sigma^2)$  reaches minimum value for the first time. For road 1, this minimal point is reached at  $\sigma = 20$ , which implies  $\hat{\sigma}_2 = 20$ . The results of combining the two methods together is also shown in Figure 2, where the values of  $\hat{\sigma}_1, \hat{\sigma}_2$  are the intersections of the blue, green vertical line and the horizontal axis separately. And blue circle points are the best estimate for noise strength, which correspond to the intersection of the green line with the horizontal axis in Figure 3. It can be seen all the best estimates for the noise strength lie in  $(\hat{\sigma}_2 - 5, \hat{\sigma}_2 + 5)$  except road 17 and 18. Therefore, the quantitative way is efficient to estimate noise strength to some degree because no assumption about noise is needed.

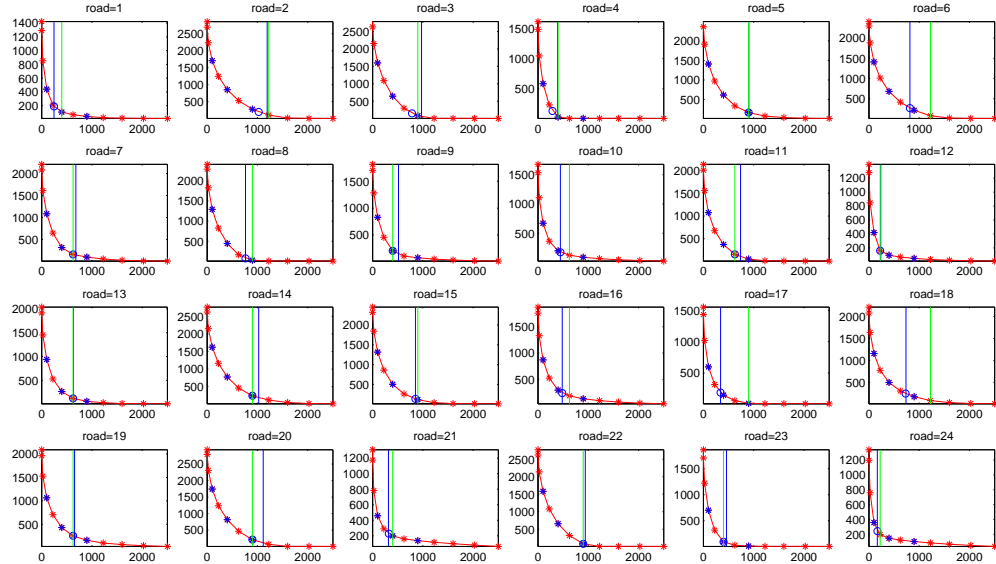


Figure 2: Relationship figure for  $TV$  and  $\sigma^2$  on Day 1.

### 3.2. Velocity before and after denoising

After choosing the best  $\sigma$  for the 24 roads, we show the velocity before and after denoising on Day 1 to observe the effect directly in Figure 4, where blue and red points represent the speed before and after denoising apart. Notice that there are missing values for many roads, so we make a nearest interpolation based on the original records and regard the velocity after interpolation as data before denoising. From Figure 4, we can say we have reduced much noise in the velocity indeed. Specifically, the speed vector is much smoother after denoising than that of before denoising. And the velocity after denoising keeps the peak values, such as the peak in the morning and evening. In addition, it can be observed when the original velocity has a sudden jump, the velocity denoised also has a jump almost at the same time, which is obviously on road 21 and 24. Namely to say, our denoising method can keep the jump when the original velocity has a sudden ascending or descending, which is very important in urban traffic prediction and analysis. This is consistent with the edge preserving property of bounded total variation method. On the other hand, the denoising effect of some roads, like road 3, 8, 22, are not that obvious as others although the performance is better than the original velocity. This may be

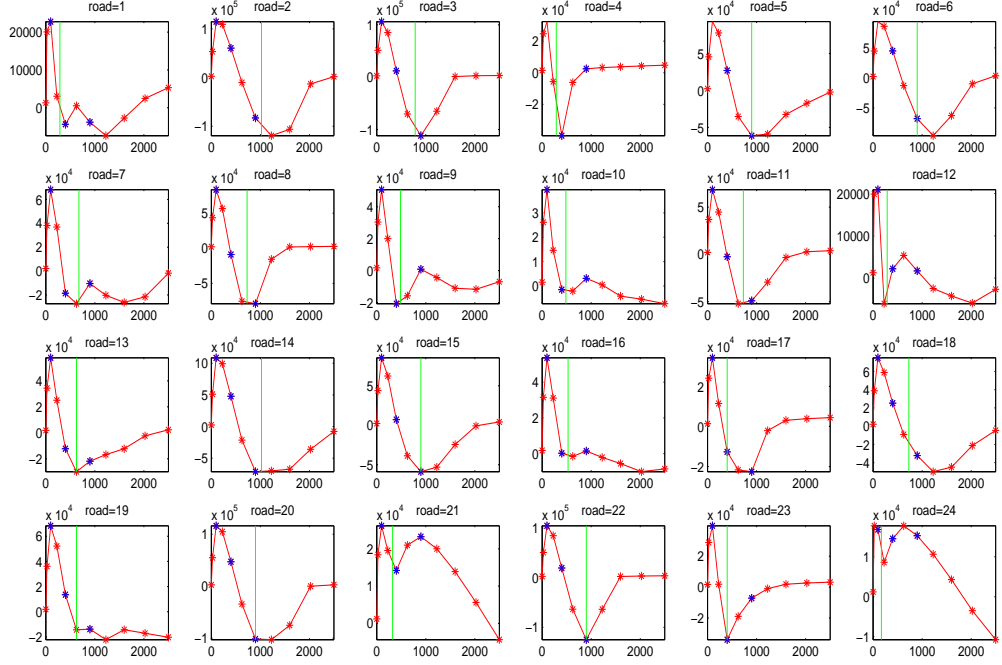
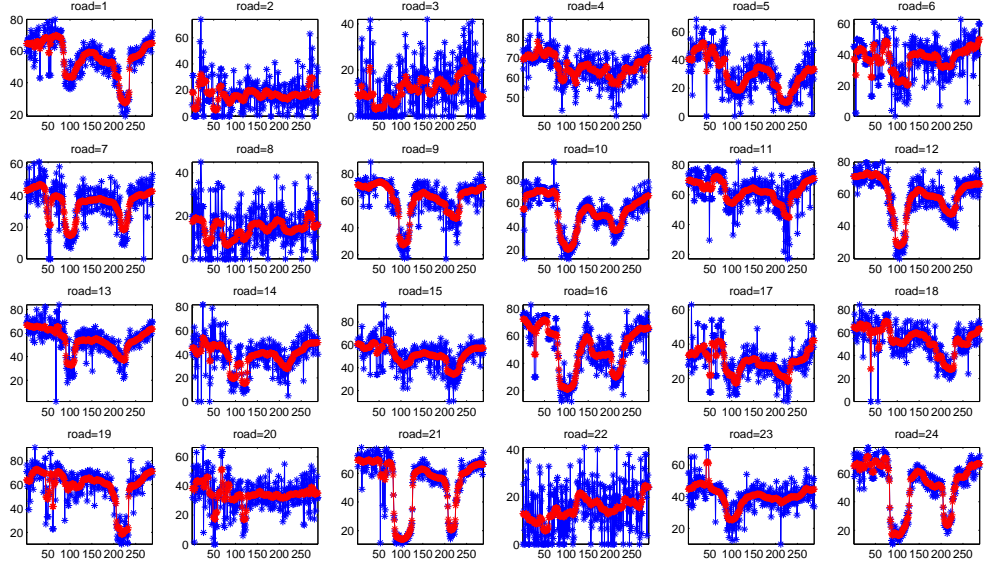


Figure 3: Estimated  $\sigma$  for the 24 roads on Day 1 with **Method 2**.

caused by their location. They are close to an intersection and are all assistant roads, which increases spatial noise, while we only consider temporal noise.



Note: The horizontal axis is 288 time slices, and the vertical axis is the velocity value.

Figure 4: Velocity before and after denoising for the 24 roads on Day 1.

### 3.3. Validation by history matching

We have seen the denoising effect directly above, then we would like to validate that this denoising method helps in velocity prediction. We first make a nearest interpolation to assure there are 288 records every day for all the chosen roads and regard the velocity after interpolation as data before denoising. Data of the first 7 days are regarded as history data, and the prediction part is from Day 8. We realize it based on history matching. Specifically, we break the history data daily into vector of length 4 in terms of time series, such that 282 vectors are obtained for each day. The first one of them is velocity record from time slice 1 to 4, and the last one is that of time slice 282 to 285. And the velocity vector after 15 minutes is from time slice 7 to 288 apart. Therefore, 1974 input vectors of length 4 and corresponding labels of length 1 are gained for the history part. And for Day 8' data, assume the current time slice is  $K$ , then the test vector is formed by velocity of time slice  $K-3$  to  $K$ . We make use of a popular clustering algorithm [27] (more details in the last part of this section) to cluster for the 1974 sample vectors and the test vector. The distance between two vectors is measured by  $l^2$  norm. After that, we regard the Gaussian-weighted average of those labels, whose input vectors are in the same cluster with the goal vector, as the velocity prediction.

What we have described is exactly the prediction process without BV denoising. For the denoising case, it is similar. For the history data, Algorithm PGDBV can be applied daily to obtain the denoised data. However, for test data from Day 8, it should be guaranteed that no future information is used to denoise and predict, leading that the denoising part should be treated carefully. Notice that a boundary condition is needed in the denoising process of Algorithm PGDBV, thus we complete a boundary value of time slice  $K+1$ , and use the velocity vector till  $K+1$  to denoise, and component of the test vector after denoising is still from  $K-3$  to  $K$ .

About completing the boundary, we use a very simple neural network based on data before denoising to make a 5-minute prediction. Input and output of the network are exactly the 1974 input vectors and corresponding labels before denoising separately. Input test are the 282 test vectors before denoising, and then the network's output test are regarded as the boundary values to denoise. Our goal is not to make a high precision prediction but to show the BV denoising functions in predicting, so relevant parameters except denoising part are not fine tuned.

We measure the predicting accuracy using relative mean absolute error (RMAE) and mean absolute percentage error (MAPE). The definitions of them are as follows:

$$\text{RMAE} = \frac{\sum_{i=1}^N |v_i - \hat{v}_i|}{\sum_{i=1}^N |v_i|}, \quad \text{MAPE} = \frac{1}{N} \sum_{i=1}^N \frac{|v_i - \hat{v}_i|}{|v_i|}.$$

Notice that when some component of the real speed vector is very close to 0, MAPE of the corresponding road will be very large. Thus we discard component whose real velocity is not bigger than 1 when calculating a road' MAPE. After obtaining the error of each chosen road, we take the average of them, which stands for the predicting error on average. 15-minute predicting results based on nearest interpolation are listed in Table 2. The RMAE reduces at least more than 1.4% when choosing  $\hat{\sigma}$  comparing with no denoising. And the MAPE reduces 2.6% with  $\hat{\sigma}$  for the chosen 24 roads on average.

Table 2: Error of 15-minute Predicting Based on Nearest Interpolation.

$\sigma$	RMAE			MAPE		
	0	$\tilde{\sigma}$	$\hat{\sigma}$	0	$\tilde{\sigma}$	$\hat{\sigma}$
average over all 24 roads	0.2641	0.2507	0.2414	0.3062	0.2803	0.2802
average w/o road 2,3,6,8,22	0.1806	0.1729	0.1660	0.2284	0.2090	0.2101
average w/o road 2,3,6,7,8,22	0.1746	0.1680	0.1605	0.2136	0.2023	0.1980

In this table, the second line represents values of  $\sigma$  applied in Algorithm PGDBV, where '0' represents the case without denoising and  $\hat{\sigma}$  means the best chosen  $\sigma$  for each chosen road, and  $\tilde{\sigma}$  means only denoising for history data with  $\hat{\sigma}$ . The third line means the average error (RMAE or MAPE) of

the 24 chosen roads. The forth line is the result of error for 19 roads except the 2nd, 3rd, 6th, 8th, 22nd roads, and the fifth line is similar. The reason why we skip road 2, 3, 6, 8, 22 is that they are rural street and the prediction accuracy is low. In addition, road 7's predicting error is also high. This may be caused by its location, which is very near to a bridge. From the predicting errors shown in these two tables, it can be seen that the RMAE is always decreased by choosing  $\sigma = \hat{\sigma}$ . This reveals  $\hat{\sigma}$  we choose for the 24 roads are appropriate and the BV denoising method we use is very useful in spirit.

We finish this section by a short discussion on interpolation for missing values. In the above, we all use the nearest interpolation to recover the missing values as it is a simple and common way. To compare the performance, we test another kind of interpolation, which is matrix completion. We find the predicting accuracy is improved a little bit compared with nearest interpolation, which indicates that the method of matrix completion is a little better than that of simple interpolation to a certain extent. Nevertheless, our goal in this paper is not predicting the velocity but exploring whether the BV denoising algorithm works well. Thus, we can use the simple nearest interpolation to finish the validation.

### 3.4. Clustering of road velocities

We randomly choose 102 roads on Day 1 and then we cluster the 102 roads according to their velocity profiles before and after denoising respectively.

When clustering, we regard the velocity of  $N$  time slices for a road as a vector whose dimension is  $N$ . As a result, we have 102 vectors in total. We measure the distance of two vectors with the  $l^2$  norm of their difference. The clustering method is based on finding of density peaks [27]. The most important reason we choose this clustering method is outliers can be discovered easily with this algorithm if exist. Outliers can be seen as noise according to [27]. Therefore, if there are outliers in the clustering result with velocity before denoising and no outliers in the clusters after denoising, we can say noise is eliminated with our denoising method. The satisfactory thing is that this is the fact, which proves the BV denoising method we use works effectively.

In order to show the process of clustering on the 102 roads in detail, it is necessary to present the procedure of clustering algorithm [27]. The steps of this clustering method combined with our data are summarized as follows:

- Step 1. Calculate the local density  $\rho_i$  for each road  $i$ :  $\rho_i = \sum_j \chi(d_{ij} - d_c)$ , where  $\chi(x) = 1$  if  $x < 0$  and  $\chi(x) = 0$  if  $x \geq 0$ ,  $d_c$  is the cutoff distance,  $d_{ij}$  is the  $l^2$  norm distance between road  $i$  and  $j$ . Let  $I_s$  denote the index set of all the 102 roads and use the Gaussian kernel to calculate  $\rho_i$ , which is defined as  $\rho_i = \sum_{j \in I_s \setminus \{i\}} \exp(-\frac{d_{ij}}{d_c})^2$ .
- Step 2. Calculate the distance to other roads with higher density for road  $i$ :  $\delta_i = \min_{j: \rho_j > \rho_i} (d_{ij})$ .
- Step 3. Plot the decision graph, in which the horizontal axis is the calculated  $\rho$  in Step 1 and vertical axis is the calculated  $\delta$  in Step 2. Points with both higher  $\rho$  and higher  $\delta$  are clustering centers. We can also plot  $\gamma (= \rho\delta)$  in decreasing order to find out the clustering centers.
- Step 4. Order all the roads' density in decreasing order. Then screen all the roads from the highest density to the lowest one. If a road is not a cluster center, then it belongs to the nearest road with higher density.
- Step 5. If the number of clusters is bigger than 1, then it's necessary to identify whether a road is a core road or a halo. Decide the border region for a fixed cluster first. Points in this region satisfy that they belong to this cluster, but there exist points belonging to other clusters within  $d_c$ . Then calculate the average local density based on the border region to identify a cluster core or halo. Outliers are often in halos.

We do as the steps above to cluster for the roads with velocity before and after denoising. From the decision graph, the first row in Figure 5, and the  $\gamma$  variance in Figure 6, we should choose 3 clusters for the 102 roads both before and after denoising. In order to observe the performance of classification obviously, we calculate the 2 dimensional non-local multidimensional scaling matrix just

as [27] does. This matrix with 2 columns is an approximation of the original distance matrix whose diagonal elements are all 0 and off-diagonal element in location  $(i, j)$  represents the distance of road  $i$  and  $j$ . The distance here refers to the  $l^2$  norm of their velocity vectors' difference. With the help of the approximated scaling matrix, we present the clustering result in the 2D non-local multidimensional scaling figure, the second row of Figure 5, where the X axis and Y axis represent the first and second column of this matrix correspondingly.

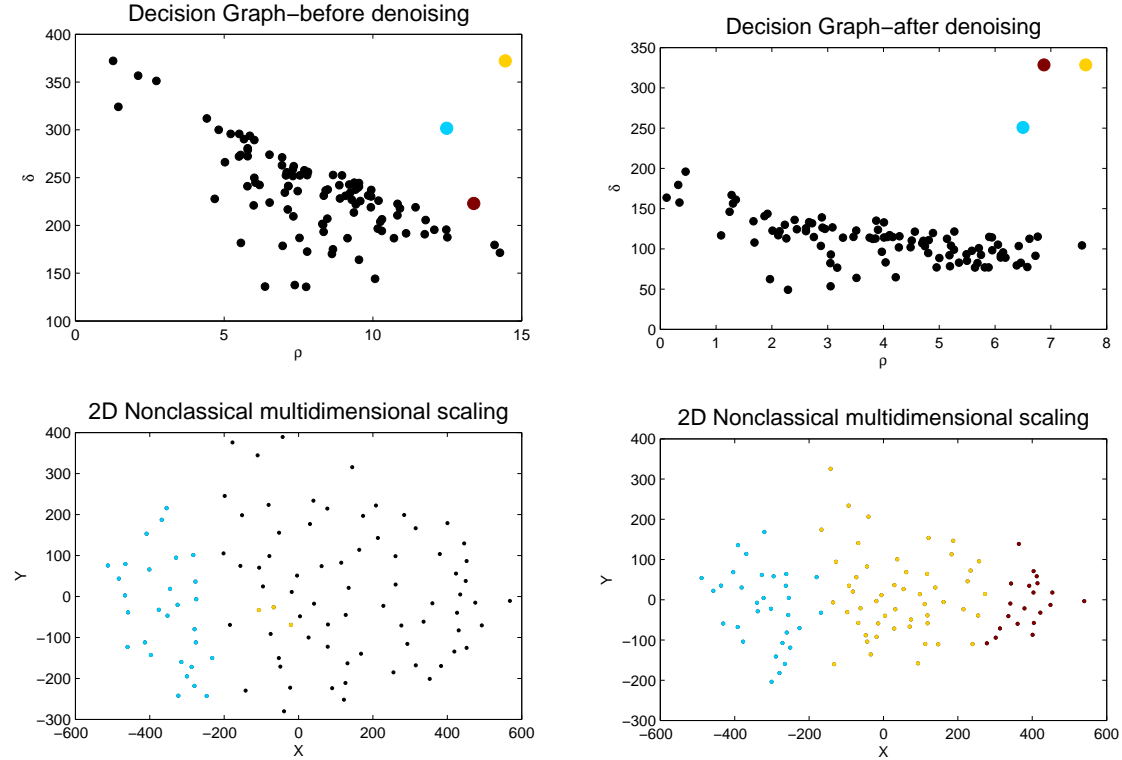


Figure 5: Decision graph and clustering result for the 102 roads.

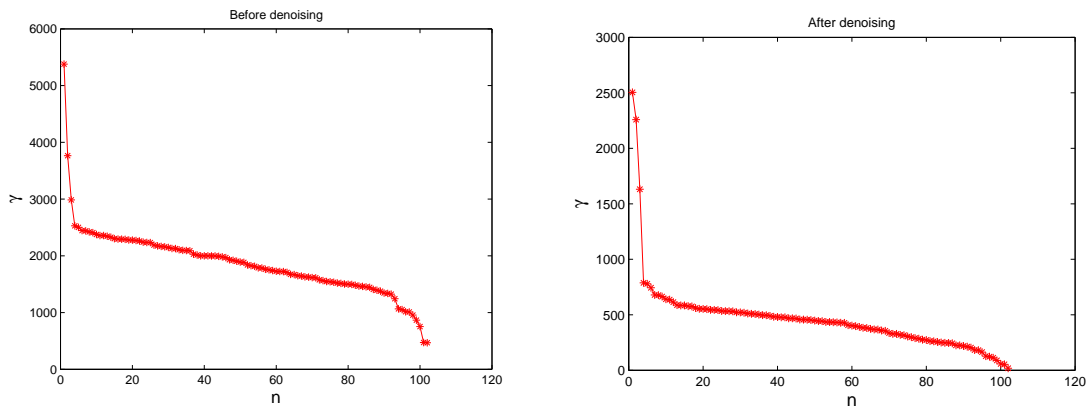


Figure 6:  $\gamma$  variance before and after denoising.

We illustrate the detailed result of clustering in the following. There are 3 points with both high  $\rho$  and high  $\delta$  in the decision graph no matter whether denoising is used, leading that 3 clusters are

chosen based on the clustering rules in [27]. The 3 cluster centers are the color points in the first row of Figure 5. The other points are shown with the color consistent in the second row of Figure 5 and classified as follows:

- 1) Before denoising, cluster 1 with 29 core elements and 0 halo corresponds to the blue points in the 2D non-local multidimensional scaling figure, and cluster 2 with 27 elements only has 3 core elements corresponding to the yellow points, and cluster 3 with 46 elements has no core elements. In the figure before denoising, if a point is a halo, then its color is black in the 2D non-local multidimensional scaling figure.
- 2) After denoising, the three clusters all have no halos. Cluster 1 has 31 core points, 29 of which are exactly the ones that in cluster 1 before denoising, and cluster 3 has 20 core points corresponding to the blue, yellow and purple points respectively in the 2D non-local multidimensional scaling figure. As there are no halos after denoising, so no black points appear this time.

Now we give some further explanations on the clustering result. In order to illustrate more clearly, we list some related numbers after BV denoising in Table 3, where line 2-4 correspond to cluster 1-3.

Table 3: Some Basic Properties of the 3 Clusters.

average velocity of cluster center	average TV of cluster center	range of velocity	range of TV
54.052	123.414	[46.165,65.398]	[56.544,259.974]
32.321	104.428	[21.967,48.021]	[95.165,482.275]
14.965	210.578	[6.396,20.641]	[118.177,239.608]

If a negative and positive linear transformation are made on average velocity and total variation apart, then the trend of variables obtained is consistent with that of X and Y in the last one of Figure 5. Therefore, cluster 1 corresponds to roads with high average velocity and relatively low total variation. Namely, they should be matched with smaller road type value, meaning that most of them are road segments on Urban Express Highway and Freeway. In fact, there are 9 roads whose type value is 1, and 17 ways whose value is 2 in cluster 1. Cluster 3 contain roads with low average speed and bigger total variation, corresponding to Prefectural Highway or Rural Street. It has been checked that all the roads' type value are 6 in cluster 3 after denoising. And cluster 2 has the medial value in terms of average speed and total variation, indicating it can contain more types of roads, which is consistent with the fact there are 8 Freeways, 15 Provincial Highways and 28 Rural Streets.

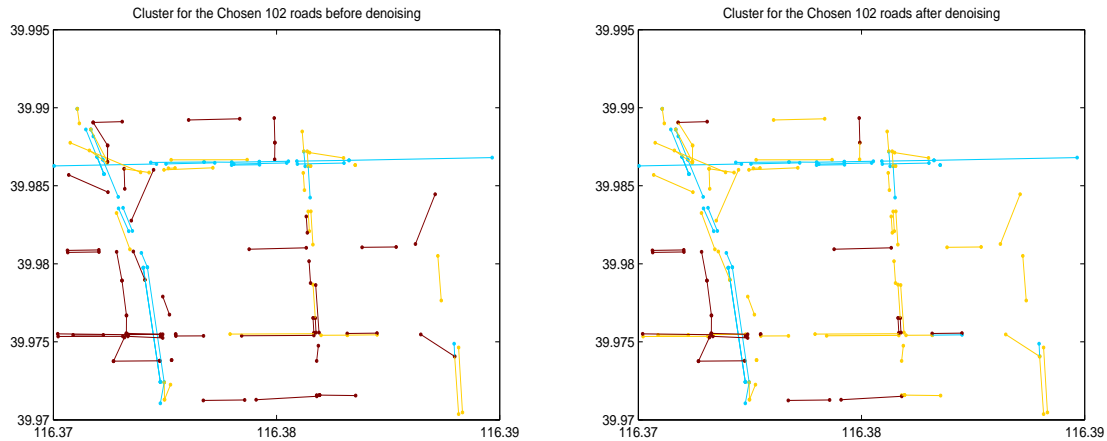


Figure 7: The clustering result matched with the original 102 roads.

Finally, in order to observe the clustering result more directly, we match the 102 points above with the original 102 roads in the color consistent and show their geographic position in Figure 7, where the horizontal axis represents longitude, and vertical axis means latitude. From this figure, we can see the clustering result after denoising is much cleaner than that before denoising. There are 28 roads belonging to different clusters before and after denoising, and most of them are rural streets. This is consistent with our common sense. By BV denoising method, these roads are discovered and the noise part is eliminated.

To summarize the clustering result, halos disappear with the BV denoising method. Because outliers often lie in halos, so we can say we obtain the clean data by denoising on the original velocity. This shows our denoising method works well.

#### 4. Conclusion and future Research

In this paper, we proposed an efficient BV denoising method for urban traffic analysis with easy-to-implement noise strength estimate algorithms. By applying the proposed BV denoising method, we have showed the road velocity prediction accuracy is improved for real urban traffic data from Beijing Taxi GPS system. We have also verified that the road clustering based on velocity profile are improved significantly by applying the BV denoising method with best noise-strength estimate.

However, in this work, we considered only the temporal characteristics of road velocity profiles, which can not deliver the full power of the denoising algorithm, since the urban road system has a very complex spatial structure. In a follow-up study, we will consider both temporal and spatial characteristics, which is more mathematically involved and will definitely give better results.

#### Acknowledgment

The authors would like to thank Beijing Transportation Information Center for providing us some valuable Taxi GPS-based data for research. The authors would also like to thank Prof. Tiejun Li, Prof. Weinan E and Dr. Yucheng Hu for helpful discussions. The work is partially supported by by China National Program on Key Basic Research Project 2015CB856003 and NNSFC 11771439.

#### References

- [1] Liu, W., Y. Zheng, S. Chawla, J. Yuan, and X. Xing, Discovering spatio-temporal causal interactions in traffic data streams. In *ACM SIGKDD International Conference on Knowledge Discovery and Data Mining*, 2011, pp. 1010–1018.
- [2] Wang, Z., M. Lu, X. Yuan, J. Zhang, and H. V. D. Wetering, Visual Traffic Jam Analysis Based on Trajectory Data. *IEEE Transactions on Visualization & Computer Graphics*, Vol. 19, No. 12, 2013, pp. 2159–2168.
- [3] Yuan, J., Y. Zheng, C. Zhang, W. Xie, X. Xie, G. Sun, and Y. Huang, T-drive: driving directions based on taxi trajectories. In *SIGSPATIAL International Conference on Advances in Geographic Information Systems*, 2010, pp. 99–108.
- [4] Kim, J. and H. S. Mahmassani, Spatial and temporal characterization of travel Patterns in a Traffic Network Using Vehicle Trajectories. *Transportation Research Part C: Emerging Technologies*, Vol. 59, 2015, pp. 375–390.
- [5] Palma, A. T., V. Bogorny, B. Kuijpers, and L. O. Alvares, A clustering-based approach for discovering interesting places in trajectories. In *ACM Symposium on Applied Computing*, 2008, pp. 863–868.
- [6] Zhan, X., Y. Zheng, X. Yi, and S. Ukkusuri, Citywide Traffic Volume Estimation Using Trajectory Data. *IEEE Transactions on Knowledge & Data Engineering*, Vol. 29, No. 2, 2017, pp. 272–285.

- [7] Brébisson, A. D., E. Simon, A. Auvolat, P. Vincent, and Y. Bengio, Artificial Neural Networks Applied to Taxi Destination Prediction. *Computer Science*, 2015.
- [8] Sadek, N. and A. Khotanzad, Multi-scale high-speed network traffic prediction using k-factor Gegenbauer ARMA model. In *Communications, IEEE International Conference on*, 2004, pp. 2148–2152 Vol.4.
- [9] Min, W. and L. Wynter, Real-time road traffic prediction with spatio-temporal correlations. *Transportation Research Part C: Emerging Technologies*, Vol. 19, No. 4, 2011, pp. 606–616.
- [10] Zhu, Y., Z. Li, H. Zhu, M. Li, and Q. Zhang, A Compressive Sensing Approach to Urban Traffic Estimation with Probe Vehicles. *IEEE Transactions on Mobile Computing*, Vol. 12, No. 11, 2013, pp. 2289–2302.
- [11] Xiao, H., H. Sun, and B. Ran, Fuzzy-Neural Network Traffic Prediction Framework with Wavelet Decomposition. *Transportation Research Record Journal of the Transportation Research Board*, Vol. 1836, No. 1, 2003.
- [12] Zheng, Z. and D. Su, Traffic state estimation through compressed sensing and Markov random field. *Transportation Research Part B Methodological*, Vol. 91, 2016, pp. 525–554.
- [13] Yarotsky, D., Error bounds for approximations with deep ReLU networks. *Neural Networks*, Vol. 94, 2017, pp. 103–114.
- [14] Liang, S. and R. Srikant, Why Deep Neural Networks for Function Approximation? *arXiv:1610.04161*, 2017.
- [15] Mahmoudi, M. and G. Sapiro, Fast image and video denoising via nonlocal means of similar neighborhoods. *IEEE Signal Processing Letters*, Vol. 12, No. 12, 2005, pp. 839–842.
- [16] Dabov, K., A. Foi, and K. Egiazarian, Video denoising by sparse 3D transform-domain collaborative filtering. In *Signal Processing Conference, 2007 European*, 2008, pp. 145–149.
- [17] Liu, C. and W. T. Freeman, *A High-Quality Video Denoising Algorithm Based on Reliable Motion Estimation*. Springer Berlin Heidelberg, 2010.
- [18] Ji, H., C. Liu, Z. Shen, and Y. Xu, Robust video denoising using low rank matrix completion. In *Computer Vision and Pattern Recognition*, 2010, pp. 1791–1798.
- [19] Rudin, L. I., S. Osher, and E. Fatemi, Nonlinear total variation based noise removal algorithms. *Physica D: Nonlinear Phenomena*, Vol. 60, No. 1, 1992, pp. 259–268.
- [20] Bao, P. and X. Ma, Image adaptive watermarking using wavelet domain singular value decomposition. *IEEE Transactions on Circuits and Systems for Video Technology*, Vol. 15, No. 1, 2005, pp. 96–102.
- [21] Baraniuk, R. G., Compressive Sensing [Lecture Notes]. *IEEE Signal Processing Magazine*, Vol. 24, No. 4, 2007, pp. 118–121.
- [22] Zheng, Z., S. Ahn, D. Chen, and J. Laval, Applications of wavelet transform for analysis of freeway traffic: Bottlenecks, transient traffic, and traffic oscillations. *Transportation Research Part B Methodological*, Vol. 45, No. 2, 2011, pp. 372–384.
- [23] Xu, D. W., H. H. Dong, H. J. Li, L. M. Jia, and Y. J. Feng, The estimation of road traffic states based on compressive sensing. *Transportmetrica B: Transport Dynamics*, Vol. 3, No. 2, 2015, pp. 131–152.
- [24] Strong, D. and T. Chan, Edge-preserving and scale-dependent properties of total variation regularization. *Inverse Problems*, Vol. 19, No. 6, 2003, pp. 165–187.

- [25] Rosen, J. B., The Gradient Projection Method for Nonlinear Programming. Part I. Linear Constraints. *Journal of the Society for Industrial & Applied Mathematics*, Vol. 9, No. 4, 1961, pp. 514–532.
- [26] Chambolle, A., V. Caselles, M. Novaga, D. Cremers, and T. Pock, An introduction to Total Variation for Image Analysis, 2009.
- [27] Rodriguez, A. and A. Laio, Clustering by fast search and find of density peaks. *Science*, Vol. 344, No. 6191, 2014, p. 1492.